Chang K, Rehermann B, McHutchison J, Pasquinelli C, Southwood S, Sette A, Chisari F (1997) Immunological significance of cytotoxic T lymphocyte epitope variants in patients chronically infected by the hepatitis C virus. J Clin Invest 100:2376–2385

Cox A, Mosbruger T, Mao Q, Liu Z, Wang X, Yang H, Sidney J, Sette A, Pardoll D, Thomas D, Ray S (2005) Cellular immune selection with hepatitis C virus persistence in humans. J Exp Med 201:1741–1752

Day C, Seth N, Lucas M, Appel H, Gauthier L, Lauer G, Robbins G, Szczepiorkowski Z, Casson D, Chung R, Bell S, Harcourt G, Walker B, Klenerman P, Wucherpfennig K (2003) Ex vivo analysis of human memory CD4 T cells specific for hepatitis C virus using MHC class II tetramers. J Clin Invest 112:831–842

Edwards P, Smith C, Neville A, O'Hare M (1982) A human–human hybridoma system based on a fast-growing mutant of the ARH-77 plasma cell leukemia-derived line. Eur J Immunol 12:641–648

Erickson A, Kimura Y, Igarashi S, Eichelberger J, Houghton M, Sidney J, McKinney D, Sette A, Hughes, A Walker C (2001) The outcome of hepatitis C virus infection is predicted by escape mutations in epitopes targeted by cytotoxic T lymphocytes. Immunity 15:883–895

Feld J, Hoofnagle J (2005) Mechanism of action of interferon and ribavirin in treatment of hepatitis C. Nature 436:967–972

Grakoui A, Shoukry N, Woolland D, Han J, Hanson H, Ghrayeb J, Murthy K, Rice C, Walker C (2003) HCV persistence and immune evasion in the absence of memory T cell help. Science 302:659–662

Huang Y, BObholzer N, Fayad R, Qiao L (2005) Turning on/off tumor-specific CTL response during progressive tumor growth. J Immunol 175:3110–3116

Imanishi T, Akaza T, Kimura A, Tokunaga K Gojobori T (1992) Allele and haplotype frequencies for HLA and complement loci in various ethnic groups. In: Tsuji K, Aizawa M, Sasazuki T (eds) The Eleventh International Histocompatibility Workshop and Conference Yokohama Japan. Oxford University Press

Kaneko T, Moriyama T, Udaka K, Hiroishi K, Kita H, Okamoto H, Yagita H, Okumura K, Imawari M (1997) Impaired induction of cytotoxic T lymphocytes by antagonism of a weak agonist borne by a variant hepatitis C virus epitope. Eur J Immunol 27:1782–1787

Karaki S, Kariyone A, Kato N, Kano K, Iwakura Y, Takiguchi M (1993) HLA-B51 transgenic mice as recipients for production of polymorphic HLA-A B-specific antibodies. Immunogenetics 37:139–142

Kimura Y, Gushima T, Rawale S, Kaumaya P, Walker C (2005) Escape mutations alter proteasome processing of major histocompatibility complex class I-restricted epitopes in persistent hepatitis C virus infection. J Virol 79:4870–4876

Kurokohchi K, Arima K, Nishioka M (2001) A novel cytotoxic T-cell epitope presented by HLA-A24 molecule in hepatitis C virus infection. J Hepatol 34:930–935

Lie W, Myers N, Gorka J, Rubocki R, Connolly J, Hansen T (1990) Peptide ligand-induced conformation and surface expression of the Ld class I MHC molecule. Nature 344:439–441

Nakamoto Y, Kaneko S, Takizawa H, Kikumoto Y, Takano M, Himeda Y (2003) Analysis of the CD8-positive T cell response in Japanese patients with chronic hepatitis C using HLA-A*2402 peptide tetramers. J Med Virol 70:51–61

Nei M, Gojobori T (1986) Simple methods for estimating the numbers of synonymous and nonsynonymous substitutions. Mol Biol Evol 3:418–426

Nielsen M, Lundegaard C, Lund O, Kesmir C (2005) The role of the proteasome in generating cytotoxic T-cell epitopes: insights obtained from improved predictions of proteasomal cleavage. Immunogenetics 57:33–41

Nouri-Aria K, ASallie R, Mizokami M, Portmann B, Williams R (1995) Intrahepatic expression of hepatitis C virus antigens in chronic liver disease. J Pathol 175:77–83

Nussbaum A, Kuttler C, Hadeler K, Rammensee H, Schild H (2001) PAProC: a prediction algorithm for proteasomal cleavages available on the WWW. Immunogenetics 53:87–94

Ray S, Fanning L, Wang X, Netski D, Kenny-Walsh E, Thomas D (2005) Divergent and convergent evolution after a common-source outbreak of hepatitis C virus. J Exp Med 201:1753–1759

Rushbrook S, Ward S, Unitt E, Vowler S, Lucas M, Klenerman P, Alexander G (2005) Regulatory T cells suppress in vitro proliferation of virus-specific CD8+ T cells during persistent hepatitis C virus infection. J Virol 79:7852–7859

Seifert U, Liermann H, Racanelli V, Halenius A, Wiese M, Wedemeyer H, Ruppert T, Rispeter K, Henklein P, Sijts A, Hengel H, Kloetzel P, Rehermann B (2004) Hepatitis C virus mutation affects proteasomal epitope processing. J Clin Invest 114:250–259

Semmo N, Day C, Ward S, Lucas M, Harcourt G, Loughry A, Klenerman P (2005) Preferential loss of IL-2-secreting CD4+ T helper cells in chronic HCV infection. Hepatology 41:1019–1028

Sugimoto K, Ikeda F, Standanlick J, Nunes F, Alter H, Chang K (2003) Suppression of HCV-specific T cells without differential hierarchy demonstrated ex vivo in persistent HCV infection. Hepatology 38:1437–1448

Tahara T, Yang S, Khan R, Abish S, Haemmerling G, Haemmerling U (1990) HLA antibody responses in HLA class I transgenic mice. Immunogenetics 32:351–360

Tanaka H, Akaza T, Juji T (1996) Report of the Japanese central bone marrow data center. Clin Transpl 139–144

Tester I, Smyk-Pearson S, Wang P, Wertheimer A, Yao E, Lewinsohn D, Tavis J, Rosen H (2005) Immune evasion versus recovery after acute hepatitis C virus infection from a shared source. J Exp Med 201:1725–1731

Thimme R, Bukh J, Spangenberg H, Wieland S, Pemberton J, Steiger C, Govindarajan S, Purcell R, Chisari F (2002) Viral and immunological determinants of hepatitis C virus clearance persistence and disease. Proc Natl Acad Sci USA 99:15661–15668

Timm J, Lauer G, Kavanagh D, Sheridan I, Kim A, Lucas M, Pillay T, Ouchi K, Reyor L, Schulze zur Wiesch J, Gandhi R, Chung R, Bhardwaj N, Klenerman P, Walker B, Allen T (2004) CD8 epitope escape and reversion in acute HCV infection. J Exp Med 200:1593–1604

Tokunaga K, Ishikawa Y, Ogawa A, Wang H, Mitsunaga S, Moriyama S, Lin L, Bannnai M, Watanabe Y, Kashiwase K, Tankaa H, Akaza T, Tadokoro K, Juji T (1997) Sequence-based association analysis of hLA class I and II alleles in Japanese supports conservation of common haplotypes. Immunogenetics 46:199–205

Tsubota A, Arase Y, Suzuki F, Suzuki Y, Akuta N, Hosaka T, Someya T, Kobayashi M, Saitoh S, Ikeda K, Kumada H (2004) High-dose interferon alpha-2b induction therapy in combination with ribavirin for Japanese patients infected with hepatitis C virus genotype 1b with a high baseline viral load. J Gastroenterol 39:155–161

Tsukiyama-Kohara K, Tone S, Maruyama I, Inoue K, Katsume A, Nuriya H, Ohmori H, Ohkawa J, Taira K, Hoshikawa Y, Shibasaki F, Reth M, Minatogawa Y, Kohara M (2004) Activation of the CK1-CDK-Rb-E2F pathway in full genome hepatitis C virus-expressing cells. J Biol Chem 15:14531–14541

Udaka K, Wiesmueller K.-H, Kienle S, Jung G, Tamamura H, Yamagishi H, Okumura K, Walden P, Suto T, Kawasaki T (2000) An automated prediction of MHC class I-binding peptides based on positional scanning with peptide libraries. Immunogenetics 51:816–828

Udaka K, Mamitsuka H, Nakaseko Y, Abe N (2002) Empirical evaluation of a dynamic experiment design method for prediction of MHC class I-binding peptides. J Immunol 169: 5744–5753

Valitutti S, Mueller S, Dessing M, Lanzavecchia A (1996) Different responses are elicited in cytotoxic T lymphocytes by different levels of T cell receptor occupancy. J Exp Med 183:1917–1921

Weiner A, Erickson A, Kansopon J, Crawford K, Muchmore E, Hughes A, Houghton M, Walker C (1995) Persistent hepatitis C virus infection in a chimpanzee is associated with emergence of a cytotoxic T lymphocyte escape variant. Proc Natl Acad Sci USA 92:2755–2759

Wherry E, Blattman J, Murali-Krishna K, vander Most R, Ahmed R (2003) Viral persistance alters CD8 T-cell immunodominance and tissue distribution and results in distinct stages of functional impairment. J Virol 77:4911–4927

Zeh H III, Leder G, Lotze M, Salter R, Tector M, Stuber G, Modrow S, Storkus W (1994) Flow-cytometric determination of peptide-class I complex formation. Identification of p53 peptides that bind to HLA-A2. Hum Immunol 39:79–86

J Med Ultrasonics (2007) 34:151–157
DOI 10.1007/s10396-007-0149-8

ORIGINAL ARTICLE

Seiji NAKANISHI · Bunzo MATSUURA
Masashi HIROOKA · Teruhisa UEDA · Tetsuji NIIYA
Shinya FURUKAWA · Masanori ABE · Yoichi HIASA
Yoshikazu KUBO · Morikazu ONJI

Clinical usefulness of quantitative evaluation of visceral fat by ultrasonography

Received: October 23, 2006 / Accepted: March 6, 2007

Abstract
Purpose. The aim of this work was to evaluate the usefulness of a proposed method for visceral fat volume assessment by ultrasonography (US) in identifying those at risk of metabolic syndrome, and also to establish the most suitable cutoff level of waist circumference for the diagnosis of visceral adiposity.
Methods. One hundred and fifty-two outpatients with metabolic diseases such as hypertension, diabetes, or dyslipidemia were studied. The total visceral fat volume (total-VFA) was measured by computed tomography (CT), the visceral fat area at the level of the umbilicus was measured by CT (CT-VFA), and the visceral fat area was also measured by US (US-VFA), as we recently proposed.
Results. Significant correlation coefficients were found between total-VFA and CT-VFA, US-VFA, and waist circumference in men but not in women. The correlation coefficient between US-VFA and waist circumference was significantly positive in men and weakly positive in women. According to receiver–operator characteristic curves, the cutoff value of waist circumference yielding the maximal sensitivity plus specificity for predicting more than 100 cm^2 of US-VFA was 85 cm in men and 84 cm in women. The change in US-VFA was significantly larger than that in waist circumference after a 6-month interval.
Conclusion. The US-measured visceral fat area is more useful than waist circumference in a clinical setting.

Keywords metabolic syndrome · visceral fat area · waist circumference · ultrasonography

S. Nakanishi · Y. Kubo
Department of Gastroenterology, Ehime National Hospital, Ehime, Japan

B. Matsuura · M. Hirooka · T. Ueda · T. Niiya · S. Furukawa · M. Abe · Y. Hiasa · M. Onji (✉)
Department of Gastroenterology and Metabology, Ehime University Graduate School of Medicine, 454 Shitsukawa, Toon 791-0295, Japan
Tel. +81-89-960-5308; Fax +81-89-960-5310
e-mail: onjimori@m.ehime-u.ac.jp

Introduction

Metabolic syndrome is one of the most important emerging health issues in the world. Metabolic syndrome results from multiple risk factors, including hypertension, glucose intolerance, dyslipidemia, and obesity. Subjects with metabolic syndrome have a two- to three-fold increased risk for cardiovascular diseases (CVD).[1–3] Recently, there have been many reports on the pathogenesis of metabolic syndrome that indicate a relationship between visceral adiposity and insulin resistance; this syndrome has been called syndrome X, the deadly quartet, insulin resistant syndrome, and visceral fat syndrome.[1,4–6]

Visceral adipose tissue, particularly mesenteric fat, is metabolically more active than subcutaneous or extraperitoneal fat.[7] Visceral fat is a source of nonesterified free fatty acids (FFA) and tumor necrosis factor alpha (TNFα), high levels of which can lead to insulin resistance in systemic fat or muscle tissues and hepatocytes.[8] An increase in insulin resistance and FFA in the portal vein and systemic circulation causes increased visceral fat and hepatic fat deposits. Therefore, the evaluation of visceral fat volume represents an important tool in assessing the risk of metabolic syndrome.

For the evaluation of visceral fat, we need to measure the total visceral fat weight or volume. Computed tomography (CT) and magnetic resonance imaging (MRI) are optical techniques for the accurate assessment of visceral fat volume. Several studies have revealed that visceral fat areas from a single scan obtained at the level of the umbilicus (approximately the level of L4 or L5) are highly correlated with the total visceral fat volume.[9–12] However, CT exposes the patient to ionizing radiation, and MRI is much more expensive than other methods.

Methods using ultrasonography (US) for the quantification of visceral fat as an alternative technique to CT or MRI have been proposed since 1990. One method involves the abdomen being sagittally scanned from the end of the sternum to the navel to estimate the maximum thickness of the peritoneal fat layer (Pmax).[13] In this method, Pmax corresponds to the visceral adiposity. However, methods involv-

ing measurement of one area of visceral fat using US require a well-trained examiner. We recently proposed a novel method of easily calculating the visceral fat volume by measurement of three areas of visceral fat using US.[14] Our method, using US, is a noninvasive and quick method producing good reproducibility rates.

Visceral fat volume is related to anthropometric parameters. Recent studies have demonstrated that among anthropometric parameters such as weight, body mass index (BMI), waist and hip circumference, and bicipital and tricipital skinfold thickness, waist circumference is most related to visceral fat volume. In Japan, a waist circumference of 85 cm in men and 90 cm in women approximates a visceral fat area of 100 cm^2 at the level of the umbilicus and is indicative of the risk of metabolic syndrome.[15]

The aim of this work was to evaluate the usefulness of our method of visceral fat volume assessment by US in identifying those at risk of metabolic syndrome, and also to establish the most suitable cutoff level of waist circumference for the diagnosis of visceral adiposity based on our US methods.

Subjects and methods

One hundred and fifty-two outpatients (88 men and 64 women) with metabolic diseases were studied in our department at Ehime National Hospital in Japan from May 2005 to October 2005. Informed consent was obtained from all patients. Body mass index (BMI) was calculated as body weight (kg) / [body height (m)]^2. Waist circumference (cm) measurement was taken as the circumference between the lowest rib and the top of the pelvis in the standing position.

Within 3 days of anthropometry, ultrasonography (US, SSD-5000, Aloka, Tokyo, Japan) and computed tomography (CT, LightSpeed Ultra 16, GE Medical System, Milwaukee, WI, USA) were performed in the supine position at the end of normal expiration after an overnight fast to evaluate abdominal fat deposition. The total visceral fat volume (total-VFA) by CT was calculated to integrate the total visceral fat areas. The visceral fat area (CT-VFA) and subcutaneous fat area (CT-SFA) at the level of the umbilicus by CT and total-VFA were estimated using National Institutes of Health (NIH) image software. The visceral fat area according to US (US-VFA) we recently proposed should be calculated as $-9.008 + 1.191 \times$ [distance between the internal surface of the abdominal muscle and the splenic vein (mm)] $+ 0.987 \times$ [distance between the internal surface of the abdominal muscle and the posterior wall of the aorta on the umbilicus (mm)] $+ 3.644 \times$ [thickness of the fat layer of the posterior right renal wall (mm)] (Fig. 1).[14] A visceral fat area of more than 100 cm^2 is widely accepted as visceral adiposity and can lead to metabolic syndrome. We plotted

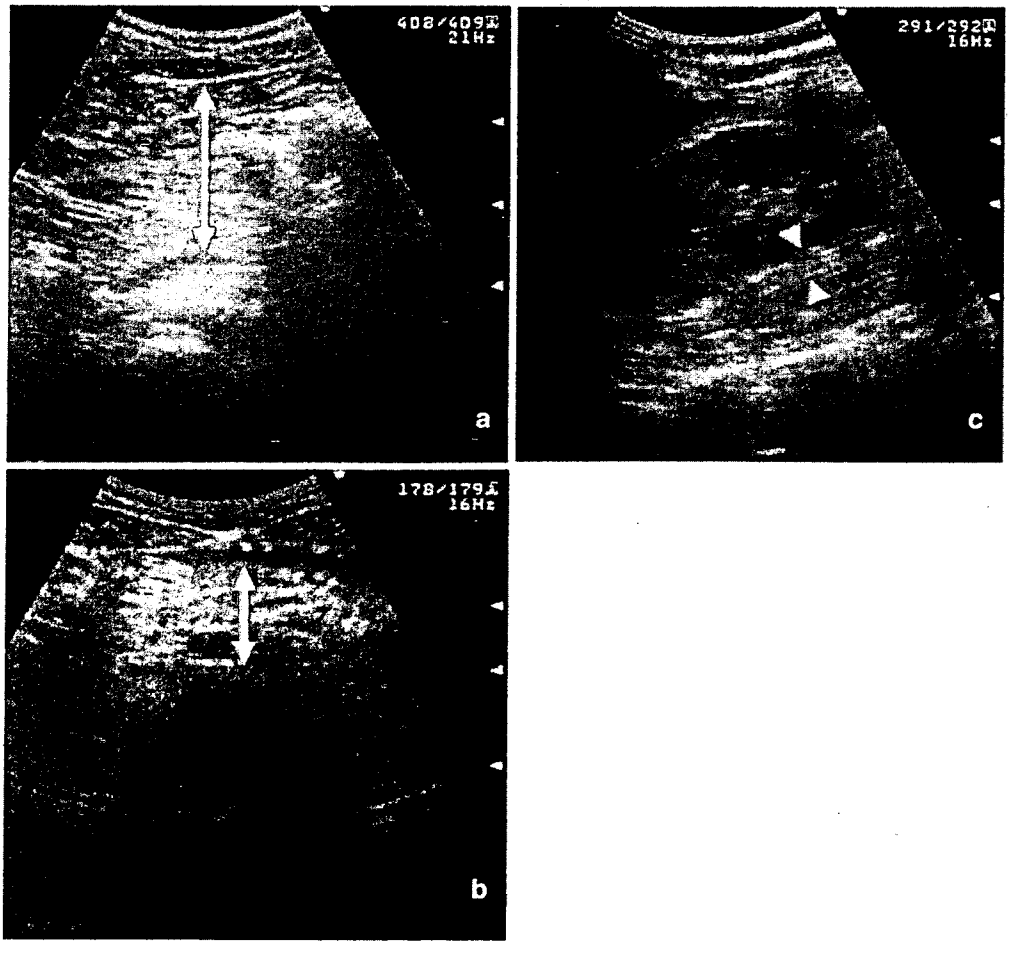

Fig. 1. Both the distance and the thickness of the parameters for visceral fat were measured by ultrasonography: **a** the distance between the internal surface of the abdominal muscle and the splenic vein (*arrow*), **b** the distance between the internal surface of the abdominal muscle and the posterior wall of the aorta on the umbilicus (*arrow*), and **c** the thickness of the fat layer of the posterior right renal wall (*arrowheads*) (modified from Hirooka et al.[14])

the receiver–operator characteristic (ROC) curves for the cutoff value of waist circumference to detect more than 100 cm^2 of US-VFA for the subjects. The inter-examiner coefficients of variation (CV) regarding the waist circumference, US-VFA, and CT-VFA measurement were 3%, 3%, and 1%, respectively, and the intra-examiner CV were 3%, 2%, and 1%, respectively.

Patients with hypertension were defined as those with systolic blood pressure ≥130 mmHg and/or diastolic pressure ≥85 mmHg. Patients with diabetes mellitus were defined as those with fasting glucose ≥126 mg/dl or glycated hemoglobin (HbA1c) ≥6.5% or those being treated. Patients with hyperlipidemia were defined as those with fasting cholesterol ≥220 mg/dl, fasting triglyceride ≥150 mg/dl, or fasting high-density lipoprotein (HDL)-cholesterol ≤40 mg/dl. Concomitant coronary heart disease was estimated as a history of angina pectoris or myocardial infarction. Concomitant cerebrovascular disease was estimated as a history of infarction by brain MRI. The following blood laboratory values were obtained in fasting conditions within 1 month of diagnosis: serum aspartate aminotransferase (AST), alanine aminotransferase (ALT), γ-glutamyl transpeptidase (γ-GTP), total cholesterol, HDL-cholesterol, triglyceride, uric acid, plasma glucose (FPG), serum insulin (IRI), and HbA1c. Insulin resistance was assessed by homeostasis model assessment of insulin resistance (HOMA-R) calculated as FPG (mg/dl) × IRI (mU/l) / 405. Twelve of the patients (7 men and 5 women) had biochemical markers, anthropometric markers, and visceral fat area prospectively measured after a 6-month interval.

All observations were expressed as means ± SD. Statistical analysis was performed using SPSS version 14 (SPSS Japan, Tokyo, Japan). Data were analyzed using the Mann-Whitney test or paired t test. Pearson's correlation coefficients were calculated to assess the association among the factors of waist circumference and visceral fat using CT and US. $P < 0.05$ was considered significant.

Results

The clinical data for all patients are shown in Table 1. Eighty-eight male patients and 64 female patients were observed. The mean age in the male group was 66 years (range, 20–84 years) and that in the female group was 65 years (range, 20–88 years). BMI, waist circumference, and biochemical markers were similar in both groups. The prevalence of hypertension, diabetes, hyperlipidemia, coronary heart disease, and cerebrovascular disease in each group was higher than that in the general Japanese population.[16]

The correlation coefficient between total-VFA and US-VFA was significantly positive ($r = 0.805$, $P < 0.0001$) (Table 2, Fig. 2), the same as we described previously.[14] A significant correlation coefficient between total-VFA and waist circumference was found in men ($r = 0.793$, $P < 0.0001$), while no correlation was found in women (Table 2).

Table 1. Clinical characteristics of the subjects in this study

	Male (n = 88)	Female (n = 64)	Total (n = 152)
Age (years)	66 ± 14	65 ± 15	65 ± 15
BMI (kg/m^2)	24.4 ± 7.5	24.6 ± 4.0	24.5 ± 6.2
Waist (cm)	85.5 ± 14.5	83.2 ± 10.0	84.5 ± 12.8
CT-VFA (cm^2)	105 ± 63	91 ± 51	99 ± 58
CT-SFA (cm^2)	103 ± 38	97 ± 40	101 ± 39
US-VFA (cm^2)	106 ± 40	89 ± 28	98 ± 36
AST (IU/l)	47 ± 34	38 ± 25	42 ± 27
ALT (IU/l)	56 ± 52	41 ± 34	50 ± 46
γ-GTP (IU/l)	38 ± 38	26 ± 26	33 ± 34
Total cholesterol (mg/dl)	167 ± 42	185 ± 48	175 ± 45
HDL-cholesterol (mg/dl)	52 ± 19	59 ± 21	55 ± 20
Triglyceride (mg/dl)	101 ± 52	108 ± 67	104 ± 59
Uric acid (mg/dl)	6.0 ± 1.5	5.3 ± 0.9	5.7 ± 1.4
FPG (mg/dl)	120 ± 55	105 ± 59	115 ± 57
FIRI (mU/l)	12 ± 5	16 ± 10	14 ± 8
HOMA-R	3.2 ± 2.0	3.8 ± 2.8	3.5 ± 2.4
HbA1c (%)	6.4 ± 2.3	6.1 ± 2.0	6.3 ± 2.2
Complications			
Hypertension (%)	35.2	20.3	28.9
Diabetes (%)	34.1	28.1	31.6
Hyperlipidemia (%)	11.4	21.9	15.8
Coronary heart disease (%)	3.4	1.6	2.6
Cerebrovascular disease (%)	1.1	1.6	1.3

Data are presented as mean ± SD

BMI, body mass index; CT-VFA, visceral fat area measured by computed tomography; CT-SFA, subcutaneous fat area measured by computed tomography; US-VFA, visceral fat area measured by ultrasonography; AST, serum aspartate aminotransferase; ALT, alanine aminotransferase; γ-GTP, γ-glutamyl transpeptidase; HDL, high-density lipoprotein; FPG fasting plasma glucose; FIRI, fasting serum immunoreactive insulin; HOMA-R, homeostasis model assessment of insulin resistance; HbA1c, glycated hemoglobin

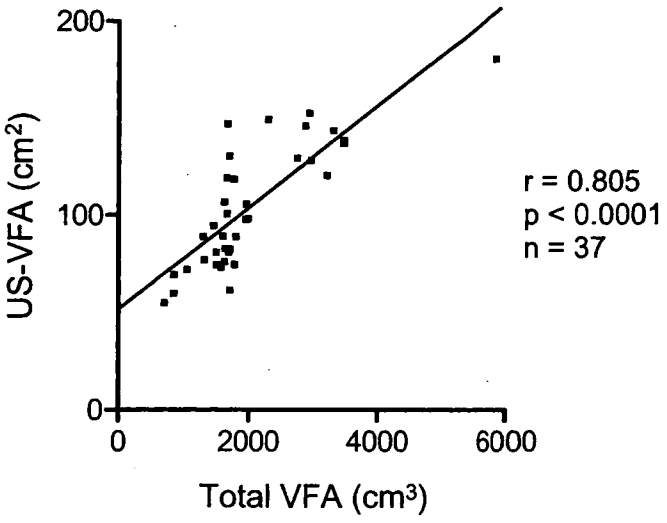

Fig. 2. Correlation between total visceral fat volume (*Total VFA*) and the visceral fat area measured by ultrasonography (*US-VFA*). A significant positive correlation was found

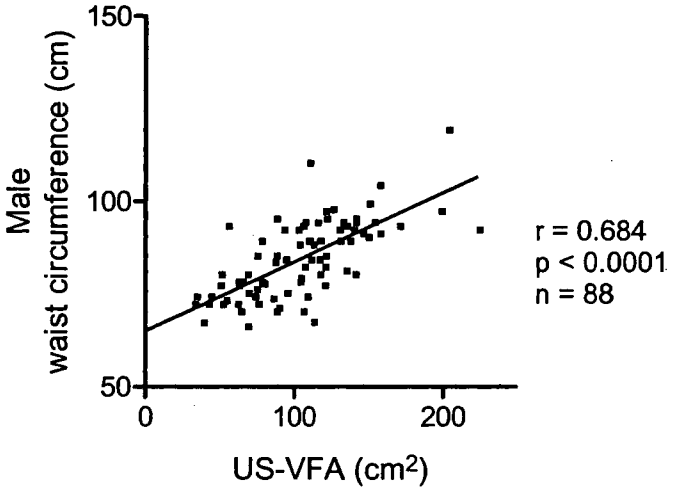

Fig. 3. Correlation between US-VFA and waist circumference in men. A significant positive correlation was found

Table 2. Correlation coefficients between total visceral fat volume and CT-VFA, US-VFA, and waist circumference

	r	p
CT-VFA (cm²)	0.840	<0.0001
US-VFA (cm²)	0.805	<0.0001
Male waist (cm)	0.793	<0.0001
Female waist (cm)	0.208	0.06

In men, the correlation coefficient between US-VFA and waist circumference was significantly positive ($r = 0.684$, $P < 0.0001$). The sensitivity and specificity of a waist circumference of 85 cm (present Japanese cutoff value) for predicting US-VFA of more than 100 cm² were 72% and 83%, respectively. According to the ROC curve, the cutoff value of waist circumference yielding the maximal sensitivity plus specificity for predicting a US-VFA of more than 100 cm²

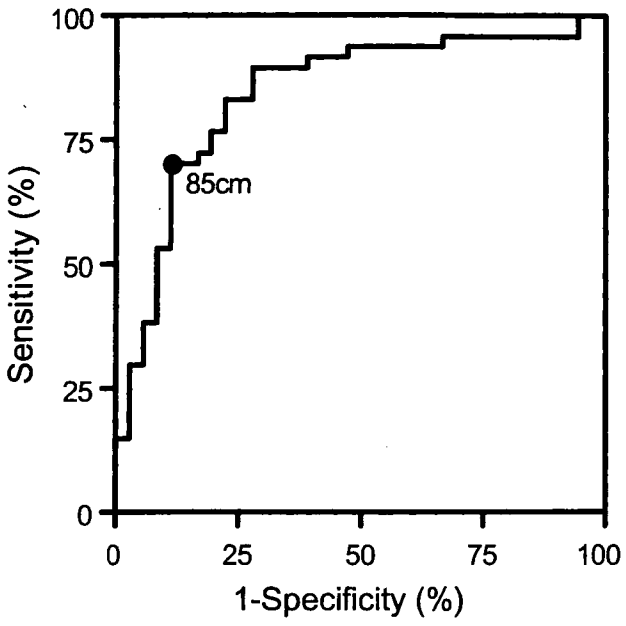

Fig. 4. The receiver–operator characteristic (ROC) curve for waist circumference to predict US-VFA of more than 100 cm² in men. *Circle*, the cutoff value of waist circumference for the present Japanese definition and for the maximal sensitivity plus specificity

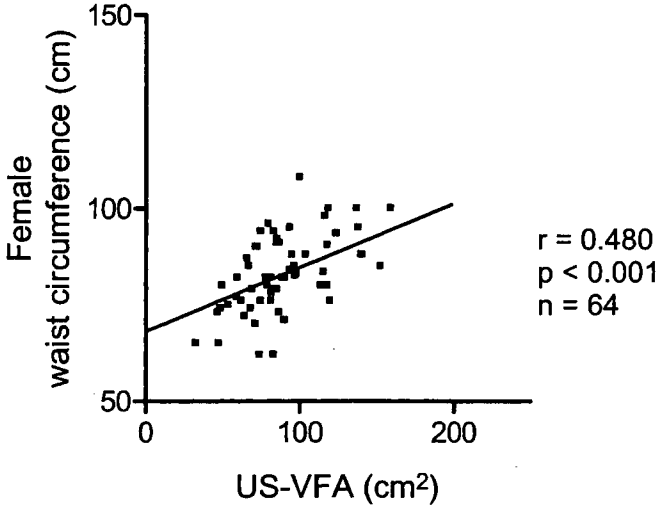

Fig. 5. Correlation between US-VFA and waist circumference in women. A weak positive correlation was found

was 85 cm (Figs. 3, 4). On the other hand, in women, the correlation coefficient between US-VFA and waist circumference was weakly positive ($r = 0.480$, $P < 0.001$). The sensitivity and specificity of a waist circumference of 90 cm (present Japanese cutoff value) for a US-VFA of more than 100 cm² were 33% and 79%, respectively. According to the ROC curve, the cutoff value of waist circumference yielding the maximal sensitivity plus specificity for a US-VFA of more than 100 cm² was 84 cm; the sensitivity and specificity were 75% and 70%, respectively (Figs. 5, 6).

We prospectively measured US-VFA and waist circumference in 12 patients (7 men and 5 women) after a 6-month

Table 3. Changes in waist circumference and US-VFA in 12 patients after a 6-month interval

Case	Sex	Age (years)	Waist circumference before (cm)	Waist circumference after (cm)	Waist circumference change (%)	US-VFA before (cm^2)	US-VFA after (cm^2)	US-VFA change (%)
1	Male	54	73	74	1	97	69	29
2	Male	66	97	94	3	127	103	19
3	Male	52	73	73	0	54	69	28
4	Male	71	84	82	2	97	88	9
5	Male	66	77	69	10	51	54	6
6	Male	82	90	94	4	105	103	2
7	Male	55	83	82	1	91	93	2
8	Female	57	87	87	0	147	113	23
9	Female	72	67	65	3	55	28	49
10	Female	60	82	72	12	90	73	19
11	Female	70	74	72	3	59	45	24
12	Female	68	74	73	1	75	84	12
Mean		64	80	78	4	87	77	18*
SD		9	9	10	4	30	26	14*

*Significant difference versus change in waist circumference ($P < 0.01$)

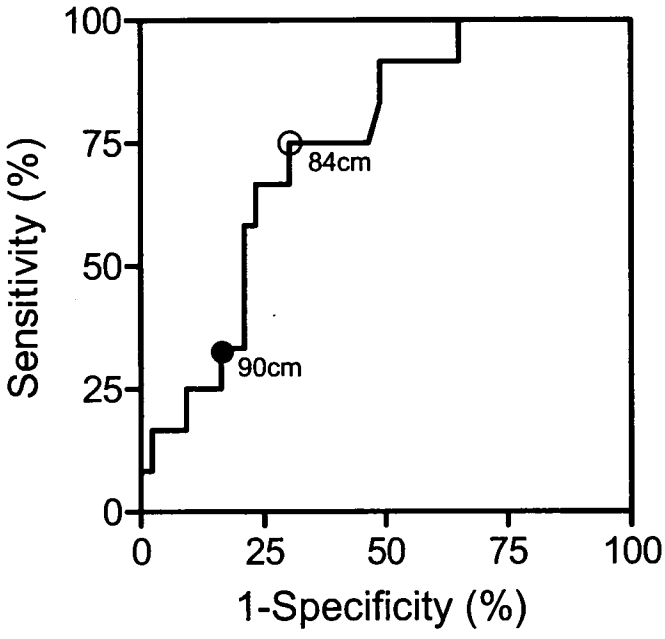

Fig. 6. The ROC curve of waist circumference to predict a US-VFA of more than 100 cm^2 in women. *Solid circle*, the cutoff value of waist circumference for the present Japanese definition; *open circle*, the cutoff value of waist circumference yielding the maximal sensitivity plus specificity

interval. The change in US-VFA was significantly larger than that in waist circumference (mean change was 18% and 4%, respectively) (Table 3).

Discussion

Recently, many studies have demonstrated that obesity is closely related to the prevalence of metabolic diseases, as is the level of visceral fat deposition.[6,17,18] Some have reported that Japanese and Caucasian subjects with a visceral fat area of more than 100 cm^2 at the umbilicus are at higher risk for diabetes and coronary heart disease.[15,19] In this way, a visceral fat area of more than 100 cm^2 at the umbilicus is widely accepted as visceral fat obesity.

There is a slight correlation between visceral fat obesity and anthropometric markers, such as weight and BMI. In patients with a BMI of more than 25 who had been considered to have visceral fat obesity, the rate of those with a visceral fat area of less than 100 cm^2 was 33%.[15] On the other hand, the prevalence of complications was high in subjects with a visceral fat area of more than 100 cm^2, even if they were not obese.[19] These results suggest that weight and BMI are not useful for the diagnosis of visceral fat obesity. Therefore, we need to measure the visceral fat area directly using abdominal images such as CT, MRI, or US. However, CT exposes the patient to ionizing radiation, and MRI is more expensive, while a method using US is noninvasive. The maximum thickness of the peritoneal fat layer (Pmax) is defined as the visceral fat volume.[13] Another method involves the abdomen being scanned within 1 cm from the umbilicus, and visceral fat is defined as the distance between the internal face of the abdominal rectal muscle and the anterior wall of the aorta.[20] We recently designed a novel method of easily calculating visceral fat volume by the measurement of three areas of visceral fat using US, significantly corresponding to the visceral fat area at the umbilicus yielded by CT.[14]

In 1997, the World Health Organization (WHO) reported that the sex-specific cutoff values of waist circumference based on data from the Netherlands for increased risk of metabolic diseases were 94 cm for men and 80 cm for women.[21] In 2000, the Steering Committee of the Western Pacific Region of WHO recommended that the cutoff values of waist circumference for Asians at high risk of metabolic diseases were 90 cm for men and 80 cm for women.[22] In 2001, the National Cholesterol Education Program's Adult Treatment Panel III (NCEP III) defined

the cutoff values of waist circumference for those at risk of metabolic diseases in the United State as 102 cm for men and 88 cm for women.[23] The Japan Society for the Study of Obesity demonstrated that in the Japanese population, the cutoff values of waist circumference corresponding to a visceral fat area of 100 cm^2 at the umbilicus (indicating a high risk of metabolic disease) according to CT was 85 cm for men and 90 cm for women.[15] The International Diabetes Federation (IDF) also reported the same values.[24,25] These cutoff values are higher in women than in men, contrary to the WHO or NCEP III criteria for Westerners or Asians. Later, some studies on the relationship between the cutoff values used for waist circumference to define visceral obesity and the rates of detection of multiple risk factors of metabolic diseases were reported. Hara et al. reported that an optimal cutoff point of waist circumference for the diagnosis of metabolic diseases in the Japanese population is 85 cm in men and 78 cm in women, yielding the maximal sensitivity plus specificity.[26] We also verified the values of waist circumference corresponding to a visceral fat area of 100 cm^2 at the umbilicus using our new method of US measurement in this study. The waist circumference is 85 cm in men, which is the same as the present Japanese definition, and 84 cm in women, which is smaller than the present Japanese definition. If the cutoff value of waist circumference is 90 cm in women, there are many false-negative cases of visceral adiposity. Further studies on the cutoff value of waist circumference are needed to define visceral fat obesity and to detect patients having multiple risk factors of metabolic syndrome. For the diagnosis of metabolic syndrome, we need exact evaluation of visceral adiposity. We think that measurement of the waist circumference is useful as a form of screening for visceral adiposity, and that our new method using US is more effective for the evaluation of visceral adiposity.

Diet- or exercise-induced weight loss is associated with a greater reduction in total body fat, preservation of lean tissue mass, and a reduction in visceral fat volume earlier than a reduction in subcutaneous fat.[27,28] In this report, we also measured changes in waist circumference and US-measured visceral fat area after a 6-month interval to assess whether the change in waist circumference reflects that of visceral fat. The change in US-VFA was significantly greater than that in waist circumference, and even in subjects whose waist circumference had not changed, the US-measured visceral fat area did change. Measurement of visceral fat area using our US method is more practical in clinics because of the low cost, the absence of side effects, and the fact that it reflects short-term change.

In conclusion, the US-measured visceral fat area is more useful in clinics compared to the waist circumference because of the early detection of short-term change in visceral fat. Also, the waist circumference corresponding to a visceral fat area of 100 cm^2 was found to be 85 cm and 84 cm in Japanese men and women, respectively.

References

1. Lakka HM, Laaksonen DE, Lakka TA, et al. The metabolic syndrome and total and cardiovascular disease mortality in middle-aged men. JAMA 2002;288:2709–16.
2. Isomaa B, Almgren P, Tuomi T, et al. Cardiovascular morbidity and mortality associated with the metabolic syndrome. Diabetes Care 2001;24:683–9.
3. Grundy SM, Brewer HB Jr, Cleeman JI, et al. Definition of metabolic syndrome: report of the National Heart, Lung, and Blood Institute/American Heart Association conference on scientific issues related to definition. Circulation 2004;109:433–8.
4. Kaplan NM. The deadly quartet: upper-body obesity, glucose intolerance, hypertriglyceridemia, and hypertension. Arch Intern Med 1989;149:1514–20.
5. Defronzo RA, Ferrannini E. Insulin resistance: a multifaceted syndrome responsible for NIDDM, obesity, hypertension, dyslipidemia, and atherosclerostic cardiovascular disease. Diabetes Care 1991;14:173–94.
6. Fujioka S, Matsuzawa Y, Tokunaga T, Tarui S. Contribution of intraabdominal fat accumulation to the impairment of glucose and lipid metabolism in human obesity. Metabolism 1987;36:54–9.
7. Ribeiro-Filho F, Faria A, Kohlmann N, et al. Two-hour insulin determination improves the ability of abdominal fat measurement to identify risk for the metabolic syndrome. Diabetes Care 2003;26:1725–30.
8. Day CP, James OF. Steatohepatitis: a tale of two hits? (editorial). Gastroenterology 1998;114:842–5.
9. Tokunaga K, Matsuzawa Y, Ishikawa K, Tarui S. A novel technique for the determination of body fat by computed tomography. Int J Obes 1983;7:437–45.
10. Busetto L, Baggio MB, Zurlo F, et al. Assessment of abdominal fat distribution in obese patients: anthropometry versus computerized tomography. Int J Obes 1992;16:731–6.
11. Dixon AK. Abdominal fat assessed by computed tomography: sex difference in distribution. Clin Radiol 1983;34:189–91.
12. de Ridder CM, de Boer RW, Seidell JC, et al. Body fat distribution in pubertal girls quantified by magnetic resonance imaging. Int J Obes 1992;16:443–9.
13. Suzuki R, Watanabe S, Hirai Y, et al. Abdominal wall fat index, estimated by ultrasonography, for assessment of the ratio of visceral fat to subcutaneous fat in the abdomen. Am J Med 1993; 95:309–14.
14. Hirooka M, Kumagi T, Kurose K, et al. A technique for the measurement of visceral fat by ultrasonography: comparison of measurements by ultrasonography and computed tomography. Intern Med 2005;44:794–9.
15. The Examination Committee of Criteria for Obesity Disease in Japan, Japan Society for the Study of Obesity. New criteria for obesity disease in Japan. Circ J 2002;66:987–92.
16. Nakamura T, Tsubono Y, Kameda-Takemura K, et al. Group of the Research for the Association between Host Origin and Atherosclerotic Diseases under the Preventive Measure for Work-related Diseases of the Japanese Labor Ministry. Magnitude of sustained multiple risk factors for ischemic heart disease in Japanese employees: a case-control study. Jpn Circ J 2001;65: 11–17.
17. Fujimoto WY, Newell-Morris LL, Grote M, et al. Visceral fat obesity and morbidity: NIDDM and atherogenic risk in Japanese-American men and women. Int J Obes 1991;15:41–4.
18. Kobayashi H, Nakamura T, Miyaoka K, et al. Visceral fat accumulation contributes to insulin resistance, small-sized low-density lipoprotein, and progression of coronary artery disease in middle-aged non-obese Japanese men. Jpn Circ J 2001;65:193–9.
19. Despres JP, Lamarche B. Effects of diet and physical activity on adiposity and body fat distribution: implications for the prevention of cardiovascular disease. Nutr Res Rev 1993;6:137–59.
20. Armellini F, Zamboni M, Rigo L, et al. The contribution of sonography to the measurement of intra-abdominal fat. J Clin Ultrasound 1990;18:563–7.
21. World Health Organization. Obesity: preventing and managing the global epidemic. Report of a WHO Consultation on Obesity. Global prevalence and secular trends in obesity. Geneva: WHO; 1997.

22. Steering Committee of the Western Pacific Region of the World Health Organization, the International Association for the Study of Obesity, and the International Obesity Task Force. The Asia-Pacific perspective: redefining obesity and its treatment. Melbourne: Health Communications Australia; 2000.
23. Expert Panel on Detection, Evaluation, and Treatment of High Blood Cholesterol in Adults. Executive summary of the Third Report of the National Cholesterol Education Program (NCEP) Expert Panel on Detection, Evaluation, and Treatment of High Blood Cholesterol in Adults (Adult Treatment Panel). JAMA 2001;285:2486–97.
24. Tan CE, Ma S, Wai D, et al. Can we apply the National Cholesterol Education Program Adult Treatment Panel definition of the metabolic syndrome to Asians? Diabetes Care 2004;27:1182–6.
25. Alberti KG, Zimmet P, Shaw J. IDF Epidemiology Task Force Consensus Group. The metabolic syndrome: a new worldwide definition. Lancet 2005;366:1059–62.
26. Hara K, Matsushita Y, Horikoshi M, et al. A proposal for the cutoff point of waist circumference for the diagnosis of metabolic syndrome in the Japanese population. Diabetes Care 2006;29:1123–4.
27. Ross R, Janssen I, Dawson J, et al. Exercise-induced reduction in obesity and insulin resistance in women: a randomized controlled trial. Obes Res 2004;12:789–98.
28. Giannopoulou I, Ploutz-Snyder LL, Carhart R, et al. Exercise is required for visceral fat loss in postmenopausal women with type 2 diabetes. J Clin Endocrinol Metab 2005;90:1511–18.

ELSEVIER

Journal of Hepatology 47 (2007) 60–66

Journal of Hepatology

www.elsevier.com/locate/jhep

Induction of anti-HBs in HB vaccine nonresponders *in vivo* by hepatitis B surface antigen-pulsed blood dendritic cells☆

Sk. Md. Fazle Akbar*, Shinya Furukawa, Osamu Yoshida, Yoichi Hiasa, Norio Horiike, Morikazu Onji

Department of Gastroenterology and Metabology, Ehime University Graduate School of Medicine, Toon City, Ehime 791-0295, Japan

***Background/Aims*: Antigen-pulsed dendritic cells (DCs) are now used for treatment of patients with cancers, however, the efficacy of these DCs has never been evaluated for prophylactic purposes. The aim of this study was (1) to prepare hepatitis B surface antigen (HBsAg)-pulsed human blood DCs, (2) to assess immunogenicity of HBsAg-pulsed DCs in vitro and (3) to evaluate the efficacy of HBsAg-pulsed DCs in hepatitis B (HB) vaccine nonresponders.**

***Methods*: Human peripheral blood DCs were cultured with HBsAg to prepare HBsAg-pulsed DCs. The expression of immunogenic epitopes of HBsAg on HBsAg-pulsed DCs was assessed in vitro. Finally, HBsAg-pulsed DCs were administered, intradermally to six HB vaccine nonresponders and the levels of antibody to HBsAg (anti-HBs) in the sera were assessed.**

***Results*: HB vaccine nonresponders did not exhibit features of immediate, early or delayed adverse reactions due to administration of HBsAg-pulsed DCs. Anti-HBs were detected in the sera of all HB vaccine nonresponders within 28 days after administration of HBsAg-pulsed DCs.**

***Conclusions*: This study opens a new field of application of antigen-pulsed DCs for prophylactic purposes when adequate levels of protective antibody cannot be induced by traditional vaccination approaches.**

***Keywords*: Anti-HBs; Dendritic cells; HB vaccine; HBsAg; HBsAg-pulsed dendritic cells; Vaccine nonresponders**

1. Introduction

Hepatitis B virus (HBV) infection is a global public health problem. Of the approximately 2 billion people who have been infected worldwide, more than 350 million are chronically infected with HBV. Although donor screening, screening of pregnant mothers, risk-reduction counseling and services, and effective infection control practices can reduce the potential risk for HBV transmission, immunization is by far the single most effective preventive measure [1,2].

Immunization with free antigens usually induces humoral antibody, however, all previous studies have shown that 5–10% of apparent healthy individuals do

Received 3 November 2006; received in revised form 11 February 2007; accepted 27 February 2007; available online 9 April 2007

☆ The authors who have taken part in this study declared that they have no relationship with the manufacturers of the drugs involved either in the past or present and did not receive funding from the manufacturers to carry out their research. The authors received funding from the Ministry of Education, Culture, Sports, Science and Technology, Japan which enabled them to carry out their study.

* Corresponding author. Tel.: +81 89 960 5308; fax: +81 89 960 5310.

E-mail address: akbar@m.ehime-u.ac.jp (S.M.F. Akbar).

Abbreviations: HBV, hepatitis B virus; HBsAg, hepatitis B surface antigen; Anti-HBs, antibody to HBsAg; HLA, human leukocyte antigen; DCs, dendritic cells; IL, interleukin; KLH, keyhole limpet hemocyanin; PBS, phosphate-buffered saline.

0168-8278/$32.00
doi:10.1016/j.jhep.2007.02.021

not produce adequate levels of protective antibody following standard immunization with HB vaccine containing free hepatitis B surface antigen (HBsAg) [3]. Moreover, the levels of antibody to HBsAg (anti-HBs) of an unknown further fraction of hepatitis B (HB) vaccinated persons fall considerably over time rendering them at potential risk of infection. The exact mechanisms underlying non responsiveness to HB vaccine are not known, however, certain human leukocyte antigen (HLA) and murine major histocompatibility complex haplotypes are related with HB vaccine non-responsiveness [4–7]. In addition, investigators have shown that immune responses to HBsAg are not properly induced in HB vaccine nonresponders due to inadequate priming of T and B lymphocytes [8,9]. A well-planned experiment by Egea et al. suggested a very specific failure of antigen presentation in HB vaccine nonresponders [10].

In this context, we paid attention to antigen-presenting dendritic cells (DCs). DCs are present in almost all tissues of the body and perform five major functions for induction of antigen-specific immune responses. These include: (1) antigen recognition, (2) antigen capture, (3) antigen internalization, (4) intracellular processing of antigens and expression of antigenic epitopes on their surface and (5) activation of lymphocytes by presenting antigenic epitopes to lymphocytes [11–14]. Several investigators have shown that it is possible to induce antigen-specific immune responses by administering antigen-pulsed DCs when that cannot be achieved by administration of free antigens or vaccines only [15–17]. In the context of HBV infection, we have shown that administration of HBsAg-pulsed DCs induced high levels of anti-HBs in HBV transgenic mice, a murine model of chronic HBV infection [18]. Although potent immune modulatory capacities of antigen-pulsed DCs have been documented in various animal models of human diseases, antigen-pulsed DCs have almost exclusively been used in patients with cancers [19]. Little is known about safety and clinical utility of antigen-pulsed DCs in non-cancerous subjects. Again, it is unknown whether antigen-pulsed DCs have any role for prophylactic purposes in humans.

Therefore, we conducted this study to open a new field of application of antigen-pulsed DCs in non-cancerous subjects and for prophylaxis purposes. HBsAg-pulsed DCs were prepared by culturing DCs from HB vaccine nonresponders with HBsAg in vitro. HBsAg-pulsed DCs were expressing immunogenic epitopes of HBsAg in vitro. Finally, HBsAg-pulsed DCs were administered to HB vaccine nonresponders to assess the safety and to evaluate the capacity of HBsAg-pulsed DCs to induce anti-HBs in HB vaccine nonresponders.

2. Materials and methods

2.1. Clinical trial design and study population

The study was an open-label, phase-1 safety and immunogenicity trial in healthy adults. The study protocol conforms to the ethical guidelines of the "Declaration of Helsinki" as reflected in a priori approval by the Institution's Human Research Committee. Six HB vaccine nonresponders were enrolled in this study: five were male and one was female. Four HB vaccine nonresponders were of Japanese origin, whereas, the rest of the two were from the Indian subcontinent. All HB vaccine nonresponders were previously immunized by HB vaccines according to standard vaccination protocol (Table 1). However, anti-HBs were not detected in the sera of these subjects (>3.0 mIU/ml). HLA haplotypes such as HLA-A, -B, -C, HLA-DR and HLA-DQ were checked in each HB vaccine responder, as shown in Table 2. HB vaccine nonresponders were apparently healthy and free from any diseases including liver and autoimmune diseases during study commencement. All HB vaccine nonresponders were negative for HBsAg and HBV DNA in the sera. Also, they were negative for HCV RNA and none of them were alcoholics. The subjects were also free from undernutrition, overnutrition and malnutrition.

Five normal subjects who were immunized with a standard course of HB vaccine and developed anti-HBs in the sera were also enrolled in this study. DCs and T cells of these HB vaccine responders were used to optimize culture conditions for production of HBsAg-pulsed DCs.

2.2. Isolation of DCs from peripheral blood and preparation of HBsAg-pulsed DCs

Cell isolation and cultures were performed in a special culture room. All reagents used for cell culture studies were free from endotoxin and toxoplasma.

Peripheral blood mononuclear cells (PBMCs) were isolated from freshly drawn heparinized whole blood by Ficoll–Hypaque (Sigma, St. Louis, MO, USA) density gradient centrifugation, washed three times, and resuspended in RPMI 1640 (Nipro, Osaka, Japan) plus 10% autologous serum.

Purified populations of T cells were isolated from PBMC by using T cell recovery kit (Collect™, Biotex Laboratories INC, Edmonton, Canada), exactly as described [20]. Flow cytometric analysis revealed that the purity of T cell populations was >95%.

To isolate DC, PBMCs were cultured in RPMI 1640 with 10% autologous sera and human grade granulocyte-macrophage colony stimulating factor (800 U/ml) and interleukin-4 (400 U/ml) (Pepro Tech EC Ltd., Margravine Road, London, UK) for 7 days, as described [20,21]. DCs were then retrieved from cultures and washed 3 times with phosphate-buffered saline (PBS).

To prepare HBsAg-pulsed DCs, human blood DCs were cultured with a commercial HB vaccine containing HBsAg (Heptavax-II, subtype adw, Banyu Pharmaceutical Co, Tokyo, Japan). After the end of cultures, DCs were pelleted and washed 5 times in PBS. The final wash solutions were collected and preserved at −20 °C to assess if there was any free HBsAg in HBsAg-pulsed DCs. To prepare keyhole limpet hemocyanin (KLH)-pulsed DCs, human blood DCs were cultured with 10 μg of KLH (Sigma, St. Louis, MO, USA) for 8 h.

2.3. Analyses of phenotype and functions of DCs

The expressions of HLA-A, -B, -C, HLA-DR, CD86, and CD40 were analyzed by direct flow cytometry using fluorochrome-conjugated monoclonal antibodies, as described [20,21]. Isotype-matched antibodies were used as controls. Data acquisition and analysis were performed on fluorescein-activated cell sorter (Becton Dickinson Biosciences, San Jose, CA, USA).

The capacities of DCs to induce proliferation of allogenic T cells were assessed in allogenic mixed leukocyte reaction in which T cells from an allogenic donor were cultured with graded doses of DCs from another normal subject.

Table 1
Clinical profile of HB vaccine nonresponders

HB vaccine nonresponders	Age/sex	Previous immunization[a]	Serum HBsAg	Serum anti-HBs	Serum HBV DNA
1.	49/Male	3 courses [5 years]	−ve	−ve	−ve
2.	30/Male	2 courses [2 years]	−ve	−ve	−ve
3.	30/Male	2 courses [1 year]	−ve	−ve	−ve
4.	52/Male	3 courses [1 year]	−ve	−ve	−ve
5.	49/Male	2 courses [1 year]	−ve	−ve	−ve
6.	45/Female	2 courses [5 years]	−ve	−ve	−ve

All HB vaccine nonresponders were healthy at the time of entry into this clinical trial. They were not suffering from any feature of generalized inflammation. Also, the parameters of liver and kidney functions were within normal range. All were negative for HBV DNA (by polymerase chain reaction), HBsAg, and anti-HBs. The estimation levels of HBsAg and anti-HBs were 0.2 ng/ml and 3 mIU/ml, respectively, by CLIA method.

[a] Immunization for one course means that the person was injected with 3 injections of vaccine containing HBsAg at 0, 1, 6 months regimen. Figures in parentheses indicate the duration from the last vaccination.

To evaluate the capacities of HBsAg-pulsed DCs to stimulate HBsAg-specific T cells, T cells from HB vaccine responders were cultured with HBsAg-pulsed DCs from the same persons.

To assess if HBsAg-specific DCs induced cellular immunity in HB vaccine nonresponponders due to immunization with HBsAg-pulsed DCs, T cells from vaccine nonresponders were cultured with HBsAg before and after administration of HBsAg-pulsed DCs.

Cultures were done for 5 days and pulsed with ^{3}[H]-thymidine (1 μCi/ml, Amersham Biosciences UK Limited, Buckinghamshire, UK) for last 16 h. The levels of incorporation of ^{3}[H]-thymidine were estimated in scintillation counter (Beckman LS 6500, Beckman Instruments, Inc, Harbor Bld, Fullerton, CA, USA) as counts per minute (cpm).

The extent of HBsAg-specific proliferation was expressed by stimulation index. Stimulation index was calculated from the following formula: cpm of cultures containing HBsAg or HBsAg-pulsed DCs divided by cpm of control cultures. Stimulation index of more than 2.0 was regarded as significant proliferation.

2.4. Immunization of HB vaccine nonresponders with HBsAg-pulsed DCs

HBsAg-pulsed DCs were suspended in PBS in two 1.0 ml syringes. In one syringe, 20 μl of PBS contained 2×10^5 HBsAg-pulsed DCs. In a second syringe, 5 million HBsAg-pulsed DCs were diluted in 250 μl of PBS. First, 2×10^5 HBsAg-pulsed DCs in 20 μl of PBS were injected at the anterior part of forelimb of HB vaccine nonresponders. After 15 min, HB vaccine nonresponders were injected with five million HBsAg-pulsed DCs, intradermally, in the deltoid region. The vaccine nonresponders were closely monitored for the first 24 h for any alteration of vital signs. Blood was collected from all HB vaccine nonresponders before and 1, 3, 7, 14, 28 and 56 days after injection with HBsAg-pulsed DCs. The blood or sera of HB vaccine nonresponders were checked for: [1] general parameters of inflammation, allergy and hypersensitivity reactions: complete blood counts including lymphocyte subsets, C-reactive protein, and serum electrolytes, [2] parameters of liver function test such as alanine aminotransferase, asparate aminotransferase, gamma-transpeptidase, lactate dehydrogenase, alkaline phosphatase, total bilirubin, direct and indirect bilirubin, and prothrombin time, [3] kidney function test such as serum creatinine and blood urea nitrogen, [4] autoantibodies such as antinuclear antibody, microsomal antibody, and thyroid antibody.

3. Results

3.1. Immunogenicity of HBsAg-pulsed DCs in vitro

In this study, we first isolated DCs from HB vaccine responders that exhibited anti-HBs in the sera due to vaccination with HB vaccines. Flow cytometric analyses revealed that human monocyte-derived blood DCs expressed DC-related surface antigens such as HLA-A, -B, -C, HLA-DR, CD86, CD40, and CD1a. The frequencies of contaminating T lymphocytes (CD3-positive cells), B lymphocytes (CD19, 20, 21-positive cells), monocytes (CD14-positive cells), and natural killer cells (CD56-positive cells) were less than 5% (data not shown). As shown in Fig. 1, DCs stimulated allogenic T cells in a dose-dependent manner.

DCs of these subjects were cultured with different amounts of HBsAg (5–30 μg) for different durations (4–48 h) to prepare HBsAg-pulsed DCs. Commercially-available HB vaccine was used as source of HBsAg. Culture of DCs with large amounts of HB vaccine (>10 μg) or for a prolonged period (>8 h) compromised the viability of HBsAg-pulsed DCs. More than 95% HBsAg-pulsed DCs were viable when DCs were cultured with 10 μg of HBsAg for 8 h. However, the viability reduced to 50–70% when DCs were cultured with 20 μg HBsAg for 16–48 h.

To assess the immunogenicity, HBsAg-pulsed DCs from vaccine responders were cultured with T cells from the same vaccine responders to assess if HBsAg-pulsed DCs were capable of induction proliferation of autologous T cells in an antigen-specific manner. As shown in Fig. 2, HBsAg-pulsed DCs stimulated HBsAg-specific T cells without addition of HBsAg in cultures.

3.2. Preparation of HBsAg-pulsed DCs from HB vaccine nonresponders

DCs were isolated from HB vaccine nonresponders exactly according to the protocol that was used to isolate DCs from vaccine responders. DCs from vaccine nonresponders were also cultured with HBsAg in a similar way to prepare HBsAg-pulsed DCs from vaccine nonresponders. The expressions of HLA-A, -B, -C, HLA-DR, CD86 and CD40 on unpulsed DC and HBsAg-pulsed DCs from a typical case of HB vaccine nonresponder are shown in Fig. 3.

Table 2
HLA-A, -B, -C and HLA-DR and -DQ of HB vaccine nonresponders

HB vaccine nonresponder-1	49/Male	HLA-A: A 24, A-33; HLA-B: B44, B75; HLA-C: CW7	HLA-DR: DR7; HLA-DQ: DQ2, DQ3
HB vaccine nonresponder-2	30/Male	HLA-A: A 24, A-26; HLA-B: B59, B62; HLA-C: CW1, CW3	HLA-DR: DR4, DR15; HLA-DQ: DQ1, DQ3
HB vaccine nonresponder-3	30/Male	HLA-A: A 2, A 24; HLA-B: B60, B61; HLA-C: CW3	HLA-DR: DR4, DR9; HLA-DQ: DQ3, DQ4
HB vaccine nonresponder-4	52/Male	HLA-A: A 2, A 24; HLA-B: B38, B46; HLA-C: CW1, CW7	HLA-DR: DR4, DR8; HLA-DQ: DQ4, DQ7
HB vaccine nonresponder-5	49/Male	HLA-A: A 2, A 24; HLA-B: B38, B46; HLA-C: CW1, CW7	HLA-DR: DR4, DR9; HLA-DQ: DQ3, DQ4
HB vaccine nonresponder-6	45/Female	HLA-A: A11, A28; HLA-B: B18, B52; HLA-C: CW7	HLA-DR: DR14, DR 15; HLA-DQ: DQ1

HB vaccine nonresponders in Japan exhibit HLA-DR4 or, HLA-DR7 or HLA-DQ4 haplotype. Vaccine nonresponder-1 and 6 are from the Indian subcontinent and HLA haplotype of HB vaccine nonresponder of that region are not known.

3.3. Assessment of safety HBsAg-pulsed DCs in HB vaccine nonresponders

There was no evidence of erythema, edema, or features of allergic or hypersensitivity reactions at the site of injection of HBsAg-pulsed DCs. This was examined immediately after injection and also periodically for 3 months. HB vaccine nonresponders did not show features of generalized inflammation or abnormal liver or kidney functions. The levels of IgM, IgG, and IgA were not increased in any HB vaccine nonresponders due to administration of HBsAg-pulsed DCs. Three HB vaccine nonresponders were positive for autoantibodies (antinuclear antibodies, thyroid autoantibodies and microsomal antibody) without any feature of autoimmune diseases. The titers of autoantibodies were not increased in any HB vaccine nonresponders due to administration of HBsAg-pulsed DCs.

3.4. Immunogenicity of HBsAg-pulsed DCs in HB vaccine nonresponders

The purpose of this clinical trial was to assess if administration of HBsAg-pulsed DCs can induce anti-HBs in HB vaccine nonresponders. All six vaccine HB nonresponders received two–three standard courses of HB vaccination prior to their entry in this pilot study. These HB vaccine nonresponders never developed anti-HBs due to HB vaccination and the levels of anti-HBs were <3.0 mIU/ml in all HB vaccine nonresponders. Interestingly, anti-HBs were detected in the sera within 28 days of administration of a single injection of HBsAg-pulsed DCs in all HB vaccine nonresponders. However, the levels of anti-HBs varied considerably among HB vaccine nonresponders (4.1–587 mIU/ml). In 3 vaccine nonresponders (#2, #3, and #6), administration of HBsAg-pulsed DCs for one time induced >10 mIU/ml of anti-HBs within 14 days of administration

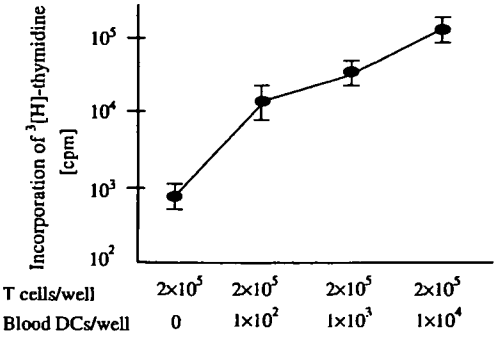

Fig. 1. Blood DCs stimulated allogenic T cells in a dose dependent manner. DCs were stimulated with allogenic T cells for 120 h and the levels of blastogenesis are expressed as counts per minutes (cpm). The mean and standard deviation of cpm of 12 wells from 3 subjects are shown.

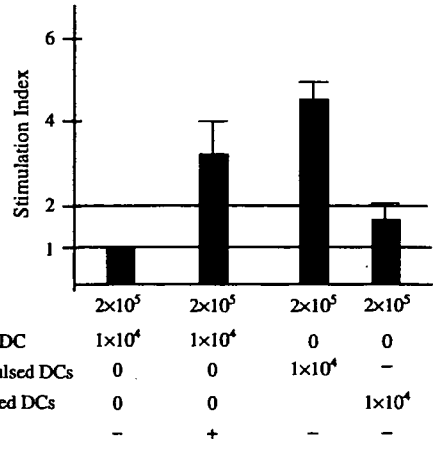

Fig. 2. HBsAg-specific DCs induced proliferation of HBsAg-specific T cells in vitro. DCs and T cells were isolated from HB vaccine responders, as described. HBsAg-pulsed DCs were prepared by culturing DCs with HBsAg. HBsAg-pulsed DCs, but not KLH-pulsed DCs, stimulated T cells from vaccine responders. The data are shown as stimulation index of 3 separate experiments (mean and standard deviation). The level of proliferation in culture containing T cells and unpulsed DCs was considered as background proliferation and expressed as stimulation index of 1.0. The levels of proliferation of stimulation index of >2.0 were regarded as significant proliferation. +, culture containing HBsAg; –, culture containing no HBsAg.

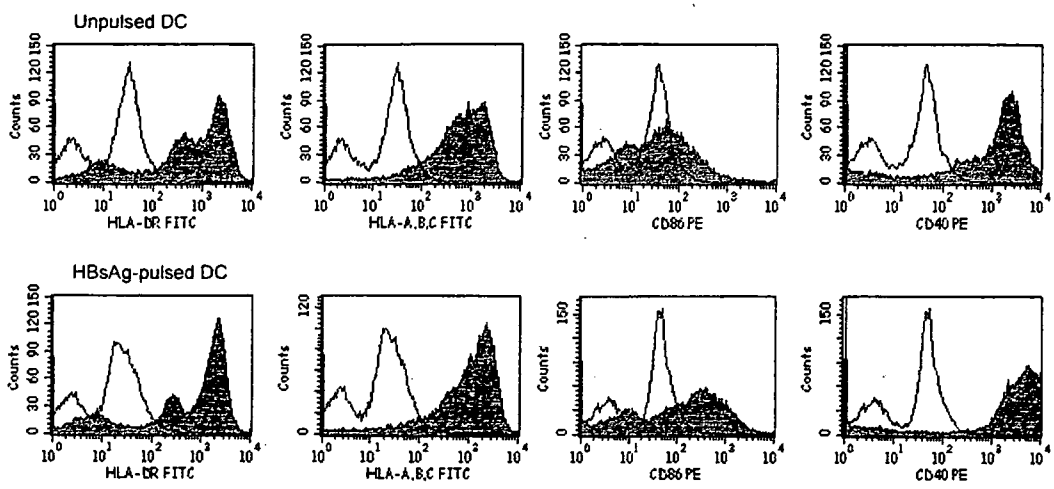

Fig. 3. Human dendritic cells (DCs) were enriched from peripheral blood of hepatitis B vaccine nonresponders by culturing peripheral blood mononuclear cells with granulocyte-macrophage colony stimulating factor and interleukin-4 (unpulsed DC) HBsAg-pulsed DCs were prepared by culturing DCs with HBsAg (10 μg) for 8 h, as described. The expression of HLA-DR, HLA-A, -B, -C, CD86 and CD40 on unpulsed DCs and HBsAg-pulsed DCs on a representative case of vaccine nonresponder (# 1 of Table 1) is shown. The unshaded area indicates the flow cytometric profile due to use of isotype control antibody, whereas, the shaded area represents the cell expansion due to usage of fluorochrome-conjugated antibodies.

of HBsAg-pulsed DCs (Table 3). The levels of anti-HBs continued to be >10 mIU/ml in two vaccine nonresponders (#2 and #6) for 90 days. The levels of anti-HBs were <10 mIU/ml but >3.0 mIU/ml in three HB vaccine nonresponders (#1, #4 and #5). These HB vaccine nonresponders were injected with HBsAg-pulsed DCs, 3 months after first immunization. The levels of anti-HBs in the sera became 51 mIU/ml (#4) and 16.4 mIU/ml (#5) in these HB vaccine nonresponders after re-immunization.

In 5 HB vaccine nonresponders (#1, #2, #3, #4, and #6), HBsAg-specific cellular immune responses were checked before and after administration of HBsAg-pulsed DCs. HBsAg-specific lymphocytes were not detected in these subjects before administration of HBsAg-pulsed DC because lymphocytes from these subjects did not proliferate due to stimulation with HBsAg in vitro (stimulation index: 1.2, 1.0, 0.8, 1.5, and 1.4 in subjects #1, #2, #3, #4, and #6, respectively). However, significant levels of HBsAg-specific cellular immune responses were detected in 4 HB vaccine nonresponders 6–8 weeks after administration of HBsAg-pulsed DCs (stimulation index of 2.8, 5.6, 3.8, 1.8, and 7.2 in subjects #1, #2, #3, #4, and #6, respectively) due to stimulation with HBsAg in vitro.

Table 3
Induction of anti-HBs in vaccine nonresponders due to immunization with HBsAg-pulsed DCs

HB vaccine nonresponders	Levels of anti-HBs (mIU/ml)			
	0	14	28	90 [DAYS][a]
1.	Undetectable	4.85	3.82	3.5
2.	Undetectable	13.6	25.9	24.1
3.	Undetectable	13.7	<30	<3.0
4.	Undetectable	<3.0	5.9	5.8
5.	Undetectable	4.1	4.2	4.2
6.	Undetectable	587	329	167

HBsAg-pulsed DCs were prepared by culturing human blood DCs with HBsAg for 8 h. The levels of anti-HBs in the sera were undetectable in all nonresponders (<3.0 mIU/ml by chemiluminescence enzyme immunoassay method) before administration of HBsAg-pulsed DCs. Five million HBsAg-pulsed DCs were injected on day 0. The levels of anti-HBs in the sera during next 90 days are shown.

[a] [DAYS] means duration after administration of HBsAg-pulsed DCs.

4. Discussion

In general, humoral immune responses are induced by administration of free antigens and commercial vaccines containing free surface antigens of the HBV are widely used for prophylaxis against the HBV. However, immunization with vaccines containing HBsAg fails to induce anti-HBs in some apparently healthy individuals. Investigators have tried to induce anti-HBs in HB vaccine nonresponders by various approaches such as (1) using HB vaccines containing HBsAg as well as preS antigens (2) administering increased amounts of antigens in vaccine and (3) injecting two or three standard courses of HB vaccines [22–26]. Recently, DNA vaccines that express HBsAg in situ have been used in HB vaccine nonresponders [27]. Here, we have shown that HBsAg-pulsed DCs, a cell-based vaccine, may be another effective tool for inducing anti-HBs in HB vaccine nonresponders.

The usage of antigen-pulsed DC is not new because several clinical trials have been conducted in which cancer antigen-loaded DCs have been used for therapeutic

purposes (for review please check reference 15). For cancer immunotherapy, tumor antigen-pulsed DCs are prepared by culturing tumor products (whole tumor, tumor mRNA, tumor lysates, or tumor fusion products) and DCs in vitro. Moreover, these ex vivo generated DCs are not usually characterized before their administration to cancer patients.

However, several important points deserve serious consideration during preparation of antigen-pulsed DCs for using in non-cancerous subjects. During the last 15 years, we prepared HBsAg-pulsed immunogenic murine spleen DCs [11,17,18], but we failed to produce HBsAg-pulsed human blood DCs based on those protocols. Prior to this clinical trial, we performed a series of experiments using DCs from normal control subjects to optimize the culture conditions for preparing immunogenic HBsAg-pulsed DCs (unpublished observations). Cultures of human DCs for 24 or 48 h or with vaccine containing 20–40 μg of HBsAg resulted in reduced viability of HBsAg-pulsed DCs, the exact causes of which have yet to be explored. In this study, we used a human consumable and the safest source of HBsAg (HBsAg in commercial vaccine) to prepare HBsAg-pulsed DCs. As HB vaccine contains HBsAg and aluminum hydroxide it is possible that HBsAg may be adsorbed to DCs during preparation of HBsAg-pulsed DCs. However, the impact of adsorbed HBsAg will be minimum, if any, in this study because there was no free HBsAg in HBsAg-pulsed DCs. Moreover, administration of HBsAg-pulsed DCs induced both anti-HBs and HBsAg-specific cellular immune responses in HB vaccine nonresponders, although previous vaccination with HB vaccine containing HBsAg for 6–9 times did not induce detectable levels of anti-HBs in these subjects. However, these points remain to be explored in future.

The mechanism underlying anti-HBs induction capacities of HBsAg-pulsed DCs in HB vaccine nonresponders is not clear. HBsAg-pulsed DCs do not undergo further processing *in vivo* and they may have directly stimulated lymphocytes for anti-HB production in HB vaccine nonresponders.

The present study is largely observational but critical to understand the safety of antigen-pulsed DCs in immune competent subjects and to assess the efficacy in nonresponders to prophylactic vaccines. Although all HB vaccine nonresponders developed anti-HBs due to a single injection of HBsAg-pulsed DCs, the levels of anti-HBs were not high. Moreover, the anti-HB levels declined with time in most HB vaccine responders. But, it should be mentioned that these HB vaccine nonresponders never produced anti-HBs after immunization with HB vaccine prior to this clinical trial. From our previous experiences in mice system, we are hopeful that it will be possible to produce more effective and immunogenic HBsAg-pulsed DCs by manipulation of culture conditions. It is also apparent that multiple injections of HBsAg-pulsed DCs may be required for sustained presence of anti-HBs in HB vaccine nonresponders. In this study, we administered 5 million HBsAg-pulsed DCs in HB vaccine nonresponders. Administration of increased amounts of HBsAg-pulsed DCs may induce higher levels of anti-HBs.

In summary, we provided a protocol of production of antigen-pulsed DCs for use in immune competent and non-cancerous humans. This is also the first study to show that antigen-pulsed DCs can be used for prophylactic purposes. This pilot study showed that HBsAg-pulsed DCs can be used to induce anti-HBs in different types of HB vaccine nonresponders including patients with hepatitis C virus infection and human immune-deficiency virus infection. The most tempting method one may adopt to induce and sustain anti-HBs in liver transplanted subjects with a HBV background. Immunizations with traditional HB vaccines have provided mixed signals about sustained anti-HB production in these subjects [28,29].

Acknowledgements

This work was supported by Grant-in-Aid for Scientific Research from the Ministry of Education, Culture, Sports, Science and Technology, Japan, to Sk. Md. Fazle Akbar (No. 17590651), and Morikazu Onji (No. 17590652).

References

[1] Lavanchy D. Hepatitis B virus epidemiology, disease burden, treatment, and current and emerging prevention and control measures. J Viral Hepat 2004;11:97–107.
[2] Alter MJ. Epidemiology and prevention of hepatitis B. Semin Liver Dis 2002;25:39–46.
[3] Hilleman MR. Critical overview and outlook: pathogenesis, prevention, and treatment of hepatitis and hepatocellular carcinoma caused by hepatitis B virus. Vaccine 2003;21:4626–4649.
[4] Milich DR, Leroux-Roels GG. Immunogenetics of the response to HBsAg vaccination. Autoimmun Rev 2003;2:248–257.
[5] Hatae K, Kimura A, Okubo R, Watanabe H, Erlich HA, Ueda K, et al. Genetic control of nonresponsiveness to hepatitis B virus vaccine by an extended HLA haplotype. Eur J Immunol 1992;22:1899–1905.
[6] Watanabe H, Okumura M, Hirayama K, Sasazuki T. HLA-Bw54-DR4-DRw53-DQw4 haplotype controls nonresponsiveness to hepatitis-B surface antigen via CD8-positive suppressor T cells. Hum Immunol 1988;22:9–17.
[7] Goncalves L, Albarran B, Salmen S, Borges L, Fields H, Montes H, et al. The nonresponse to hepatitis B vaccination is associated with impaired lymphocyte activation. Virology 2004;326:20–28.
[8] Jarrosson L, Kolopp-Sarda MN, Aguilar P, Bene MC, Lepori ML, Vignaud MC, et al. Most humoral non-responders to hepatitis B vaccines develop HBV-specific cellular immune responses. Vaccine 2004;22:3789–3796.
[9] Krishnamurthy G, Kher V, Naik S. Low response to HBsAg vaccine in chronic renal failure patients is not due to intrinsic defect of B cells. Scand J Urol Nephrol 2002;36:377–382.

[10] Egea E, Iglesias A, Salazar M, Morimoto C, Kruskall MS, Awdeh Z, et al. The cellular basis for lack of antibody response to hepatitis B vaccine in humans. J Exp Med 1991;173:531–538.
[11] Akbar SMF, Furukawa S, Horiike N, Onji M. Vaccine therapy for hepatitis B virus carrier. Curr Drug Targets Infect Disord 2004;4:93–101.
[12] Steinman RM, Pope M. Exploiting dendritic cells to improve vaccine efficacy. J Clin Invest 2002;109:1519–1526.
[13] Mellman I, Steinman RM. Dendritic cells: specialized and regulated antigen processing machines. Cell 2001;106:255–258.
[14] Banchereau J, Steinman RM. Dendritic cells and the control of immunity. Nature 1998;392:245–252.
[15] Mocellin S, Mandruzzato S, Bronte V, Lise M, Nitti D. Part I: vaccines for solid tumours. Lancet Oncol 2004;5:681–689.
[16] Onji M. Dendritic cells in clinics. Tokyo: Springer; 2004.
[17] Akbar SMF, Murakami H, Horiike N, Onji M. Dendritic cell-based therapies in the bench and the bed sides. Curr Drug Targets Inflamm Allergy 2004;3:305–310.
[18] Akbar SMF, Furukawa S, Hasebe A, Horiike N, Michitaka K, Onji M. Production and efficacy of a dendritic cell-based therapeutic vaccine for murine chronic hepatitis B virus carrier. Int J Mol Med 2004;14:295–299.
[19] Sheng KC, Pietersz GA, Wright MD, Apostolopoulos V. Dendritic cells: activation and maturation – applications for cancer immunotherapy. Curr Med Chem 2005;12:1783–1800.
[20] Arima S, Akbar SMF, Michitaka K, Horiike N, Nuriya H, Kohara M, et al. Impaired function of antigen-presenting dendritic cells in patients with chronic hepatitis B: localization of HBV DNA and HBV RNA in blood DC by in situ hybridization. Int J Mol Med 2003;11:169–174.
[21] Ninomiya T, Akbar SMF, Masumoto T, Horiike N, Onji M. Dendritic cells with immature phenotype and defective function in the peripheral blood from patients with hepatocellular carcinoma. J Hepatol 1999;31:323–332.
[22] Bonanni P, Bonaccorsi GBonanni P, Bonaccorsi G. Vaccination against hepatitis B in health care workers. Vaccine 2001;19:2389–2394.
[23] Leroux-Roels G, Desombere I, Cobbaut L, Petit MA, Desmons P, Hauser P, et al. Hepatitis B vaccine containing surface antigen and selected preS1 and preS2 sequences. 2. Immunogenicity in poor responders to hepatitis B vaccines. Vaccine 1997;15:1732–1736.
[24] Kim MJ, Nafziger AN, Harro CD, Keyserling HL, Ramsey KM, Drusano GL, et al. Revaccination of healthy nonresponders with hepatitis B vaccine and prediction of seroprotection response. Vaccine 2003;21:1174–1179.
[25] Belloni C, Tinelli C, Orsolini P, Pistorio A, Avanzini A, Moretta A, et al. Revaccination against hepatitis B virus of non-responding and low-responding infants immunised at birth. A parallel evaluation of rubella and tetanus vaccine. Vaccine 1998;16: 399–402.
[26] Zuckerman JN, Zuckerman AJ, Symington I, Du W, Williams A, Dickson B, et al. Evaluation of a new hepatitis B triple-antigen vaccine in inadequate responders to current vaccines. Hepatology 2001;34:798–802.
[27] Rottinghaus ST, Poland GA, Jacobson RM, Barr LJ, Roy MJ. Hepatitis B DNA vaccine induces protective antibody responses in human non-responders to conventional vaccination. Vaccine 2003;21:4604–4608.
[28] Sanchez-Fueyo A, Rimola A, Grande L, Costa J, Mas A, Navasa M, et al. Hepatitis B immunoglobulin discontinuation followed by hepatitis B virus vaccination: a new strategy in the prophylaxis of hepatitis B virus recurrence after liver transplantation. Hepatology 2000;31:496–501.
[29] Angelico M, Di Paolo D, Trinito MO, Petrolati A, Araco A, Zazza S, et al. Failure of a reinforced triple course of hepatitis B vaccination in patients transplanted for HBV-related cirrhosis. Hepatology 2002;35:176–181.

J Gastroenterol 2007; 42:306–311
DOI 10.1007/s00535-006-1949-0

Journal of Gastroenterology

Percutaneous ultrasound-guided radiofrequency ablation of hepatocellular carcinoma with artificially induced pleural effusion and ascites

Takahide Uehara, Masashi Hirooka, Kiyotaka Ishida, Atsushi Hiraoka, Teru Kumagi, Yoshiyasu Kisaka, Yoichi Hiasa, and Morikazu Onji

Department of Gastroenterology and Metabology, Ehime University Graduate School of Medicine, Shitsukawa, Toon, Ehime 791-0295, Japan

Background. Ultrasound-guided procedures are sometimes of limited use because the tumor is located under the diaphragm or near the surface of the liver. We investigated the safety and efficacy of radiofrequency ablation (RFA) with artificial pleural effusion and/or artificial ascites. ***Methods.*** Between January 2002 and May 2006, 43 lesions in 36 patients with hepatocellular carcinoma (HCC) were treated by RFA with artificial pleural effusion and/or artificial ascites. ***Results.*** Artificial pleural effusion allowed visualization of the whole tumor for 36 (83.7%) of the 43 lesions that were otherwise not detectable or poorly visible. Artificial ascites was also helpful in visualizing whole tumors that could not be visualized with only artificial pleural effusion. In all lesions, artificial pleural effusion and/or artificial ascites were helpful in performing percutaneous RFA. Artificial ascites was useful for creating a space between the liver's surface and the skin or diaphragm to avoid burns. Adverse effects after the induction of artificial pleural effusion included pneumonia in one patient and temporary atelectasis in another patient. Severe side effects were not observed. Complete necrosis after RFA was obtained in 43 (100%) of the 43 lesions. During a mean follow-up period of 31.8 ± 5.8 months, local recurrence at the ablation site was found in none of the 43 lesions. ***Conclusions.*** Percutaneous RFA with artificial pleural effusion and/or artificial ascites was a safe and useful treatment that resulted in good local control of HCC.

Key words: artificial pleural effusion, artificial ascites, radiofrequency ablation

Received: June 14, 2006 / Accepted: December 19, 2006
Reprint requests to: M. Onji

Introduction

The recent widespread use of percutaneous radiofrequency ablation (RFA) has yielded good results in the treatment of hepatocellular carcinoma (HCC).[1–3] However, when the tumor is located under the hepatic dome, it is difficult to visualize on ultrasound (US) owing to the presence of pulmonary air; thus, percutaneous tumor ablation (PTA) using thoracoscopic[4] or computed tomography (CT)-guided[5] approaches is used to overcome this limitation. As well, a laparoscopic approach has been used for tumors located near the liver's surface.[6] However, these approaches are much more invasive or complicated than PTA with artificial pleural effusion or artificial ascites. Although PTA with artificial pleural effusion[7–9] or artificial ascites[10–11] has been previously reported, there are no reports of PTA done with the combination of artificial pleural effusion and artificial ascites. Therefore, in this paper, we report our experience with and the impact of RFA for HCC done using artificial pleural effusion and artificial ascites, both separately and in combination.

Subjects and methods

Patients

Between January 2002 and May 2006, 29 men and 7 women with HCC (43 HCC lesions) were enrolled for RFA treatment with artificial pleural effusion and/or artificial ascites (Table 1). During the same period, we treated 118 patients with 263 HCC lesions by conventional RFA without combination effusion. We generally perform RFA with artificial pleural effusion or artificial ascites if the HCC nodules are located at the liver's surface, or near the diaphragm, intestine, gall bladder, stomach, or heart). Median patient age was 70.5 years (range, 48 to 89 years). All patients had longstanding

Table 1. Summary of results in patients treated by radiofrequency ablation with artificial pleural effusion and/or artificial ascites

	Age (years) median ± SD	Sex M:F	Average size (mm) mean ± SD	Number of nodules	Visualization good:poor	Complete necrosis	Local recurrence	Complications
Pleural effusion only	69.3 ± 5.9	15:2	17.3 ± 6.7	21	2:19	21	0/21	2/21 Pneumonia, 1 Liver abscess, 1
Pleural effusion and ascites	71.6 ± 4.1	11:5	13.0 ± 1.0	19	0:19	19	0/19	1/19 Atelectasis
Ascites only	69.5 ± 0.5	3:0	16.8 ± 4.8	3	3:0	3	0/3	0/3
Total	70.5 ± 4.7	29:7	16.9 ± 5.5	43	5:38	43	0/43	3/43

chronic liver disease. Three patients were positive for hepatitis B surface antigen, 30 were positive for hepatitis C virus, and three had cryptogenic hepatitis. Twenty-nine patients had Child-Pugh class A, and seven had Child-Pugh class B liver cirrhosis. Patients with Child-Pugh class C liver cirrhosis, bleeding tendency, chronic heart disease, or chronic pulmonary disease were excluded from this study. The diameter of the HCC ranged from 5 to 36 mm (mean ± standard deviation, 16.9 ± 5.5 mm) on dynamic CT (Light Speed Ultra 16, GE Yokogawa Medical Systems, Tokyo, Japan) or US (SSD 5500, Aloka, Tokyo, Japan). The ethics committee of our university approved the study protocol, and written informed consent was obtained from all patients before treatment. This study's observation period was 31.8 ± 5.8 months (range, 17.7–50.4 months).

Of the 43 lesions, 11 lesions were new and 32 were recurrent. The diagnosis of HCC was based on the presence of enhancement on CT hepatic arteriography and a perfusion defect on CT arterial portography during angiography (Integris BV 3000, Philips, Tokyo, Japan); histological findings of the percutaneous liver biopsy; and increased levels of tumor markers, such as α-fetoprotein or des-γ-carboxyprothrombin.

When a hypervascular tumor was noted on angiography, it was mandatory to perform transcatheter arterial embolization (TAE) before RFA therapy by injecting iodized oil (lipiodol, Guerbet, Paris, France) with a gelatin sponge (Gelfoam, Upjohn, Kalamazoo, MI, USA) into the segmental branch or the subsegmental branch of the hepatic artery. In this study, TAE was attempted in 31 (72.1%) of the 43 lesions.

When the tumors were located under the hepatic dome and could not be visualized or were only partly detected on US, though not on CT, US was performed again with artificial pleural effusion.

Artificial pleural effusion and artificial ascites

All patients were premedicated with an intramuscular injection of 25 mg of hydroxyzine and 15 mg of pentazocine while conscious. During each procedure, oxygen saturation and other vital signs were observed regularly.

To produce the artificial pleural effusion, the location of the pleural cavity was first determined. In practice, we identified the region considered to be the pleural cavity on US as the area where the liver could be observed on deep expiration but could not be observed on deep inspiration because of pulmonary air. This area was usually located between the right anterior and the right posterior axillary lines. After local anesthesia was given, a 21-gauge needle was inserted gently through the chest wall. When the tip of the needle was just in front of the surface of the liver, 5 to 10 ml of 5% glucose sterile solution at 37°C was injected. The needle was considered to be correctly inserted into the pleural cavity when no resistance was noted during the test injection. After approximately 5 mm of fluid space was observed on US, 50 to 100 ml of 5% glucose was injected. The needle was then changed to a 14-gauge needle (Daimon needle, Silux, Kawaguchi, Japan), and 5% glucose was rapidly injected to produce an artificial pleural effusion. After injecting a sufficient amount of 5% glucose, we attempted to observe the tumor on US with the patient in a semisitting position. More 5% glucose was added until the tumor or the needle tract was visualized clearly (Fig. 1).

Artificial ascites was produced by first establishing local anesthesia and then inserting a 21-gauge needle just in front of the surface of the liver to inject 5% glucose. RFA therapy was started as soon as the fluid space was made, before the fluid could escape into the rest of the abdomen (Fig. 2).

Radiofrequency ablation

After these procedures were completed, RFA was performed. The locations of the 43 lesions and their treatments were as follows: for 19 (8 in segment 7 and 11 in segment 8) that were located under the hepatic dome but deeper than 5 mm from the liver surface and not

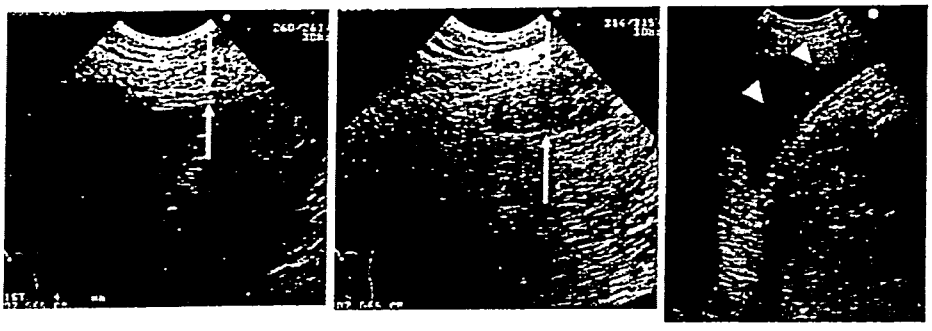

Fig. 1A–C. Production of artificial pleural effusion. **A** We found the pleural cavity (*arrows*) on ultrasound (US). A 21-gauge needle was inserted gently through the chest wall. **B** An approximately 5-mm-wide fluid space (*arrows*) was observed on US, and was followed by injection of 50 to 100 ml of 5% glucose. **C** 5% glucose was added until the tumor or the needle tract was visualized clearly by artificial pleural effusion (*arrowheads*)

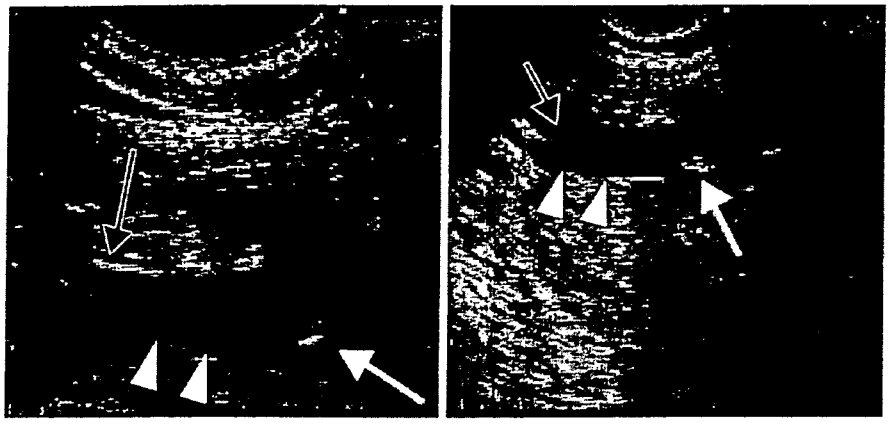

Fig. 2. Production of artificial ascites. Artificial ascites (*white arrowheads*) was produced by insertion of a 21-gauge needle (*white arrow*) into the space between the diaphragm (*black arrow*) and the surface of the liver and injecting 5% glucose. We started radiofrequency ablation therapy as soon as the fluid space was made, so that the fluid would not escape to other spaces in the abdomen

well visualized owing to the presence of pulmonary air, RFA was performed with only artificial pleural effusion being induced; for two that were well visualized on US, artificial pleural effusion was induced to obtain a safe needle tract to avoid injuring the hepatic vein; for three (1 in segment 1, 1 in segment 5, and 1 in segment 6) that were not under the hepatic dome but were located near the liver's surface (within 5 mm), RFA was performed with only artificial ascites; for 17 that were located under the hepatic dome and near the liver's surface (2 in segment 2, 8 in segment 7, and 7 in segment 8), RFA was performed with a combination of artificial pleural effusion and ascites; and for two (both in segment 8) that were not close to the liver's surface but could not be visualized well with only artificial pleural effusion, RFA was performed with a combination of an artificial pleural effusion and artificial ascites. The main factor that necessitated the use of artificial ascites or artificial pleural effusion was the location of the HCC. For HCC close to the surface of the liver, artificial ascites appeared to be better to avoid burning the pleura or peritoneum. By using artificial fluids, pain can be avoided and the HCC can be well visualized, which allows safe and precise RFA treatment.

A Cool-Tip needle radiofrequency system (Radionics, Burlington, MA, USA) was used in this study. Under US guidance, a 17-gauge monopolar Cool-Tip needle was precisely inserted into the tumor via the 14-gauge needle that was used to induce the artificial pleural effusion. In each lesion, to obtain a safety margin around the viable tumor, we selected a 2-cm or 3-cm ablation-type needle. Each ablation was done for 12 min or for at least four power roll-offs, as recommended by the manufacturer.

Within a week after RFA, dynamic CT was done. In patients in whom the low-density area surrounding the original tumor was considered large enough, "complete necrosis" of the tumor was considered to have been obtained, and no further treatment was given. However, if a low-density area did not completely surround the original tumor area, then additional RFA sessions were given until complete necrosis was achieved. When a residual tumor was easily detected on CT but it was difficult to distinguish the viable area from the original RFA ablation area on conventional gray-scale US, virtual US was used during the additional RFA treatment.

After each RFA treatment with artificial pleural effusion, as much as possible of the fluid in the pleural

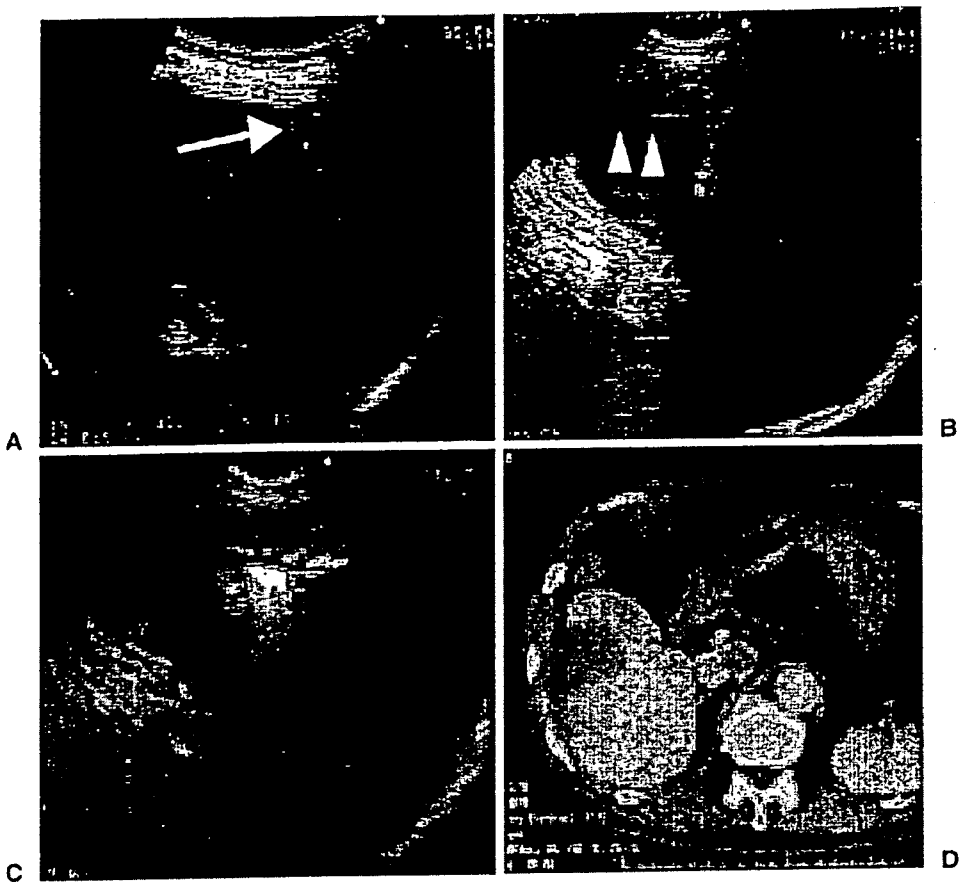

Fig. 3A–D. A 69-year-old man with hepatocellular carcinoma was treated by radiofrequency ablation with artificial ascites. **A** Ultrasonography obtained before treatment showed a hypoechoic nodule (*arrow*). **B** After an injection of 5% glucose to cause the artificial ascites (*arrowheads*), the radiofrequency ablation needle was inserted. **C** Ablation was completed without burning the diaphragm. **D** After the treatment, a computed tomography scan revealed a completely necrotic area

cavity was removed. Chest radiography was done immediately if the patient complained of respiratory symptoms, such as dyspnea or cough.

Results

Artificial pleural effusions were successfully induced in all patients; the volume (mean ± SD) of the injected pleural effusion was 514 ± 106 ml. Artificial pleural effusion allowed the visualization of the whole tumor on US in 36 (83.7%) of the 43 lesions located under the hepatic dome that were not previously detectable or were poorly visible on US. Oxygen inhalation was needed during the procedure in 5 (12.2%) of 36 patients. The pleural effusion disappeared within 1 week in 38 (95.0%) of 40 cases; one of the remaining patients developed transient pneumonia, and the other developed temporary atelectasis secondary to the artificially induced pleural effusion. One patient who received RFA with artificial pleural effusion developed a liver abscess that required drainage (Table 1).

In all lesions, artificial ascites induced with 210 ± 86 ml of 5% glucose created a space between the liver surface and skin or diaphragm that helped avoid burns. RFA treatment with artificial ascites alone was done to ablate a tumor located in segment 6 near the surface of the liver in one case; the patient's tumor developed complete necrosis without pain or skin burn (Fig. 3).

The use of artificial pleural effusion and/or artificial ascites was also helpful for visualizing the whole tumor and the needle tract in five lesions in which the conventional route was blocked by the hepatic vein. Overall, artificial pleural effusion and/or artificial ascites played a role in performing percutaneous RFA in 38 (88.4%) of the 43 lesions. In five lesions that were difficult to detect on US, virtual US was used. Among 19 patients who received RFA with artificial pleural effusion and artificial ascites, 12 patients (63.2%) experienced no pain; slight pain was reported by six patients (31.6%), and only one patient (5.2%) experience a moderate level of pain and needed analgesics. Finally, there was no lesion for which ablation had to be discontinued owing to intolerable pain. No side effects were observed in patients in whom both artificial pleural effusion and artificial ascites were induced.

Complete necrosis after RFA was obtained in 43 (100%) of the 43 lesions. Local recurrence at the ablation site was found in 0 (0%) of the 43 lesions. There were no cases of seeding in either the pleural or abdominal cavity.

During the observation period, two patients (5.5%) died from recurrent HCC and liver failure that was not related to the RFA treatment.